

THE BEZIER CURVE AS A FUZZY MEMBERSHIP FUNCTION SHAPE*

Tania Yankova[†] Galina Ilieva[‡] Stanislava Klisarova[§]

Abstract

Membership functions are a key concept in fuzzy set theory and their correctness and precision are essential for the accuracy of obtained results. This article discusses the use of Bezier curve to construct a membership function. Based on the frequency distribution of data by minimization, the coordinate formulas of the control points that define the curve are derived. Use of the described membership function is illustrated by an example. These formulas are applied to bispectral index data sets in order to compare with other published method.

MSC: 03E72, 65D05, 65D10, 65D15

keywords: Fuzzy set, Membership function, Bezier curve, Least-squares minimization

*Accepted for publication on March 5, 2018

[†]tsv1@uni-plovdiv.bg Faculty of Economics and Social Sciences, University of Plovdiv Paisii Hilendarski, 24 "Tzar Assen" str., Plovdiv, Bulgaria

[‡]galili@uni-plovdiv.bg Faculty of Economics and Social Sciences, University of Plovdiv Paisii Hilendarski, 24 "Tzar Assen" str., Plovdiv, Bulgaria

[§]stanislava.belcheva@gmail.com Faculty of Economics and Social Sciences, University of Plovdiv Paisii Hilendarski, 24 "Tzar Assen" str., Plovdiv, Bulgaria

1 Introduction

The fuzzy set theory was first introduced by Lotfi Zadeh in the 1960s as a way to capture uncertainty and vagueness often overlooked in complex systems. It can be considered as a generalization of classical set theory. Constructing fuzzy rules and building a proper membership function have been challenges for several decades by now.

The fuzzy membership function is a key concept in designing fuzzy systems. Proper and precise use of the membership function is essential for the accuracy of obtained results. Therefore, construction a membership function and determining its parameters continues to be a current issue that many researchers are focused on and have been proposing new approaches and algorithms in recent years. For example, Wu and Chen in [16] created an algorithm for developing membership functions based on α -cuts of equivalence relations and induced the fuzzy rules from the numerical training data set. Yang and Bose [17] introduced automatic fuzzy membership generation with unsupervised learning where the proper cluster is generated and then the fuzzy membership function is generated according to this cluster. Feng, Li and Hu [3] suggested a training algorithm for Hierarchical Hybrid Fuzzy-Neural Networks, based on Gaussian membership function. Viattchenin, Tati and Damaratski [15] presented the problem of constructing Gaussian membership functions derived from the data by using heuristics algorithm of possibilistic clustering. Hasuike, Katagiri and Tsubaki [5] suggested that an appropriate membership function algorithm integrate the fuzzy Shannon entropy with a piecewise linear function into subjective intervals estimation by heuristic method. Jain and Khare [8] presented a mechanism for generating membership functions that exploits the properties of Bezier curves.

For the construction of membership functions by numerical data set, Nasibov and Ulutagay in [10] used Gaussian function. Later Nasibov and Peker in [11] suggest using another exponential function as a better option for solving the same task and prove its advantage. The idea of this study was born by [11] and consists in constructing a membership function through approximation of a frequency distribution by a Bezier curve.

The rest of the paper is organized as follows: Section 2 consists of two parts. In 2.1, basic concepts of fuzzy sets theory are outlined briefly. In 2.2, the approach and results of previous research related to the present study are described. In Section 3, formulas for determining the coordinates of the Bezier curve control points are derived. Section 4 presents an algorithm for building a membership function via the Bezier curve base on the frequency distribution points and specifies an analytical expression of the proposed

membership function. The frequency distributions published in [11] are used to illustrate the proposed method. In Section 5, the described function is compared to the exponential function of Nasibov and Peker [11]. Some summaries have been made and guidelines for future research have been identified.

2 A brief preliminary

2.1 Some basic concepts of fuzzy sets theory

The concepts and principles of fuzzy sets theory can be found in [1, 7, 12, 18]. Definitions of the some basic notions used in the following presentation will be briefly listed here.

Let X be a collection of objects and $x \in X$. A fuzzy set A in X is the set of ordered pairs $A = \{(x, \mu_A(x)) \mid x \in X\}$, where $\mu_A(x): X \rightarrow T \subseteq [0, 1]$ is called a membership function for the fuzzy set A .

If $\sup \mu_A(x) = 1$, then A is called normal fuzzy set. If $\sup \mu_A(x) < 1$, then A is subnormal.

The support of A is the subset of points of X at which $\mu_A(x)$ is positive, i.e. $\text{support}(A) = \{x \in X \mid \mu_A(x) > 0\}$.

For any $\alpha > 0$, $\alpha \in T \subseteq [0, 1]$, an α -cut or α -level of the fuzzy set A in X is the set $A^\alpha = \{x \mid x \in X, \mu_A(x) \geq \alpha\}$.

The fuzzy set A is convex if and only if for any $x_1, x_2 \in X$ and any $\lambda \in [0, 1]$ is fulfilled:

$$\mu_A(\lambda x_1 + (1 - \lambda)x_2) \geq \min\{\mu_A(x_1), \mu_A(x_2)\}. \quad (1)$$

A fuzzy number A is a fuzzy set in the real line \Re with the membership function $\mu_A(x): \Re \rightarrow [0, 1]$ that satisfies the conditions for normality, convexity and piecewise continuity and $\text{support}(A)$ is bounded.

Remark 1 For a fuzzy number, the convexity defined by (1) means that the membership function is monotonic or that it is first monotonically increasing and then monotonically decreasing.

2.2 Publications related to this research

The choice of membership function type is determined by the ability of the shape of its graph to approximate with sufficient accuracy the shape of the frequency distribution of x_1, x_2, \dots, x_N data.

Nasibov and Ulutagay [10] recorded bispectral index data during sleep and analyzed it by using the Fuzzy c-Means and Fuzzy Neighborhood DB-SCAN algorithms. As a result of these computational experiments, Nasibov and Ulutagay concluded that FN-DBSCAN method gives more realistic results in recognizing stable duration intervals and bispectral index stages in the measurement series.

Remark 2 *Bispectral index scale is a continuous processed electroencephalogram parameter that correlates to the level of brain activity. The numerical value of bispectral index varies from 0 (no cerebral activity) to 100 (fully awake patient) [10].*

Sedation is the depression of the human’s awareness to environment and the reduction of responsiveness to external stimulation.

Data from the formed sedation stages in [10] and used in [11] contain the frequencies of the class intervals of a bispectral index. With some changes to the parameter markings, the overall data type is presented in Table 1.

The total number of classes in Table 1 is l . The midpoints $m_i, i = \overline{1, l}$ of the class intervals and the frequencies $f_i, i = \overline{1, l}$ are filled in the table. The relative frequencies are $p_i = \frac{f_i}{N}, i = \overline{1, l}$, where $N = \sum_{i=1}^l f_i$. The class interval with a maximum frequency:

$$p_M = \max_{i=\overline{1, l}}\{p_i\}$$

and its midpoint $m = m_M$ are determined. The normalized frequencies are $\tilde{p}_i = \frac{p_i}{p_M}, i = \overline{1, l}$, such as $\tilde{p}_M = 1$.

Class interval	Midpoint m_i	Frequency f_i	Relative frequency p_i	Normalized frequency \tilde{p}_i
$[x_0, x_1)$	$m_1 = \frac{x_0+x_1}{2}$	f_1	$p_1 = \frac{f_1}{N}$	$\tilde{p}_1 = \frac{p_1}{p_M}$
$[x_1, x_2)$	$m_2 = \frac{x_1+x_2}{2}$	f_2	$p_2 = \frac{f_2}{N}$	$\tilde{p}_2 = \frac{p_2}{p_M}$
...
$[x_{l-1}, x_l)$	$m_l = \frac{x_{l-1}+x_l}{2}$	f_l	$p_l = \frac{f_l}{N}$	$\tilde{p}_l = \frac{p_l}{p_M}$
Total		N	1	

Table 1: Frequency table

Tables 4-8 of Appendix section are filled in with numerical values and have the same appearance as Table 1. Each one corresponds to one of the five stages of sedation.

For the bispectral index values at each stage, Nasibov and Ulutagay [10] construct a Gaussian fuzzy membership function of the type:

$$\mu_A(x) = e^{-\frac{1}{2}\left(\frac{x-m}{\sigma}\right)^2} \quad (2)$$

where m (in the article the original symbol is α) is the mean value of the data, and σ is their standard deviation.

Later, Nasibov and Peker [11], solving a classification problem, suggested instead of (2) to use the following exponential membership function:

$$\mu_A(x) = \begin{cases} e^{-(\frac{x-m}{\sigma})^{s_L}}, & x \leq m \\ e^{-(\frac{x-m}{\beta})^{s_R}}, & x > m \end{cases} \quad (3)$$

with unknown parameters s_L, σ, s_R, β . They output the formulas for the unknown parameters by least squares minimization. Then they verified the efficiency of the proposed exponential membership function with respect to the bispectral index data. Based on 21 sets of bispectral data, each of which containing 306 measurements, Nasibov and Peker [11] determined the classification accuracies based on exponential membership functions (3) and Gaussian membership functions (2). They calculated the classification accuracy as the ratio of the number of correctly detected points in the data set to the total number of points in the set. By the paired t-test ($\alpha = 0,10$), they come to the conclusion that the mean of classification accuracy, based on exponential membership functions (3) is greater than the one based on Gaussian membership functions (2).

3 Approximation of a series of points by a Bezier curve

The Bezier curve is a parametric curve that is determined by a set of control points C_0, C_1, \dots, C_k . The number of control points determines the order of the curve as at $(k + 1)$ control points the curve is of order k . The curve is defined:

$$B(t) = C_0(1-t)^2 + C_12(1-t)t + C_2t^2, \text{ at } k = 2 \quad (4)$$

$$B(t) = C_0(1-t)^3 + C_13(1-t)^2t + C_23(1-t)t^2 + C_3t^3, \text{ at } k = 3 \quad (5)$$

$$B(t) = C_0(1-t)^4 + C_1 4(1-t)^3 t + C_2 6(1-t)^2 t^2 + C_3(1-t)t^3 + C_4 t^4, \quad \text{at } k=4, \quad (6)$$

where $t \in [0, 1]$. The beginning and end of the curve are coincident with the first and last control point, respectively, i.e. $B(0) = C_0$ and $B(1) = C_k$.

Let in the plane be given $(n+1)$ consecutive points $P_i(x_i, y_i), i = \overline{0, n}$ (Figure 1). Let us denote with r_i the length of the line between two adjacent points P_{i-1} and P_i , i.e.:

$$r_i = |P_{i-1}P_i| = \sqrt{(x_i - x_{i-1})^2 + (y_i - y_{i-1})^2}, i = \overline{1, n} \quad (7)$$

and assume $r_0 = 0$.

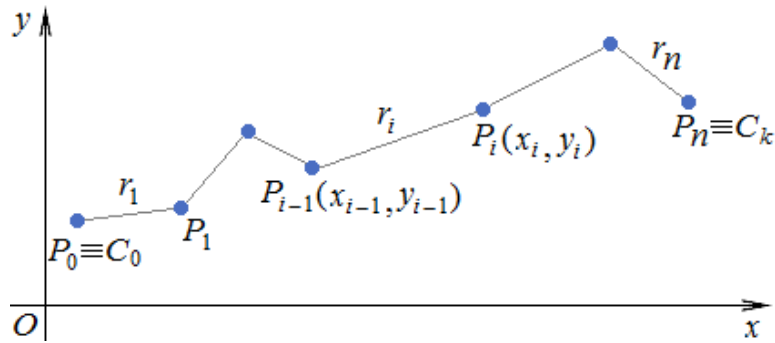


Figure 1: Series of $(n+1)$ points in the plane and the marks associated with them

The total length of the broken line that is obtained from all segments is $d_n = \sum_{i=0}^n r_i$. The length of the broken line between P_0 and P_i is $d_i = \sum_{j=0}^i r_j$.

At each point $P_i(x_i, y_i), i = \overline{0, n}$ we match quantity:

$$t_i = \frac{d_i}{d_n} \in [0, 1], i = \overline{0, n} \quad (8)$$

If we treat t_i as values of the parameter $t \in [0, 1]$, then $t = 0$ corresponds to the first point P_0 of the series of points and $t = 1$ corresponds to the last point P_n .

For $n \geq 4$ we will produce the formulas for determining the coordinates of the internal control points $C_1(C_{1x}, C_{1y}), C_2(C_{2x}, C_{2y}), C_3(C_{3x}, C_{3y})$ of the fourth-order Bezier curve, and set requirement $C_0(C_{0x}, C_{0y}) \equiv P_0(x_0, y_0)$

and $C_4(C_{4x}, C_{4y}) \equiv P_n(x_n, y_n)$. For this purpose, we will minimize the squares of the deviations of the curve from the abscisses and the ordinates of the points P_1, P_2, \dots, P_{n-1} :

$$E(C_x) = \sum_{i=1}^{n-1} (x_i - B_x(t_i))^2 \rightarrow \min \tag{9}$$

$$E(C_y) = \sum_{i=1}^{n-1} (y_i - B_y(t_i))^2 \rightarrow \min \tag{10}$$

where $B_x(t_i)$ and $B_y(t_i)$ are obtained from (6) using respectively the abscisses $C_{0x}, C_{1x}, C_{2x}, C_{3x}, C_{4x}$ and the ordinates $C_{0y}, C_{1y}, C_{2y}, C_{3y}, C_{4y}$ of the control points.

Theorem 1 For each set of points $P_i(x_i, y_i), (n \geq 4)$ in the plane, for $C_0(C_{0x}, C_{0y}) \equiv P_0(x_0, y_0)$ and $C_4(C_{4x}, C_{4y}) \equiv P_n(x_n, y_n)$, there exist singular internal control points $C_1(C_{1x}, C_{1y}), C_2(C_{2x}, C_{2y}), C_3(C_{3x}, C_{3y})$ of the fourth-order Bezier curve for which the sums $E(C_x)$ and $E(C_y)$ defined by (9) and (10) assume their minimum values.

Proof: Let's first look at only the abscisses of the points. From (9) and (6) there is obtained:

$$\frac{\partial E(C_x)}{\partial C_x} = 2 \sum_{i=1}^{n-1} (x_i - B_x(t_i)) \frac{\partial B_x(t_i)}{\partial C_x} = 0$$

Let we denote:

$$S_{p,q} = \sum_{i=1}^{n-1} (1 - t_i)^p t_i^q ; \tag{11}$$

$$SX_{p,q} = \sum_{i=1}^{n-1} x_i (1 - t_i)^p t_i^q ; \tag{12}$$

$$SY_{p,q} = \sum_{i=1}^{n-1} y_i (1 - t_i)^p t_i^q ; \tag{13}$$

$$S_{(4)} = \begin{bmatrix} 4S_{6,2} & 6S_{5,3} & 4S_{4,4} \\ 4S_{5,3} & 6S_{4,4} & 4S_{3,5} \\ 4S_{4,4} & 6S_{3,5} & 4S_{2,6} \end{bmatrix}.$$

Then the resulting system:

$$\begin{cases} C_{1x} 4S_{6,2} + C_{2x} 6S_{5,3} + C_{3x} 4S_{4,4} = SX_{3,1} - C_{0x}S_{7,1} - C_{4x}S_{3,5} \\ C_{1x} 4S_{5,3} + C_{2x} 6S_{4,4} + C_{3x} 4S_{3,5} = SX_{2,2} - C_{0x}S_{6,2} - C_{4x}S_{2,6} \\ C_{1x} 4S_{4,4} + C_{2x} 6S_{3,5} + C_{3x} 4S_{2,6} = SX_{1,3} - C_{0x}S_{5,3} - C_{4x}S_{1,7} \end{cases}$$

has the solution:

$$\begin{bmatrix} C_{1x} \\ C_{2x} \\ C_{3x} \end{bmatrix} = S_{(4)}^{-1} \begin{bmatrix} SX_{3,1} - C_{0x}S_{7,1} - C_{4x}S_{3,5} \\ SX_{2,2} - C_{0x}S_{6,2} - C_{4x}S_{2,6} \\ SX_{1,3} - C_{0x}S_{5,3} - C_{4x}S_{1,7} \end{bmatrix}. \quad (14)$$

Similarly, from (10) and (6) for the ordinates of the three control points we obtain:

$$\begin{bmatrix} C_{1y} \\ C_{2y} \\ C_{3y} \end{bmatrix} = S_{(4)}^{-1} \begin{bmatrix} SY_{3,1} - C_{0y}S_{7,1} - C_{4y}S_{3,5} \\ SY_{2,2} - C_{0y}S_{6,2} - C_{4y}S_{2,6} \\ SY_{1,3} - C_{0y}S_{5,3} - C_{4y}S_{1,7} \end{bmatrix}. \quad (15)$$

The matrix $S_{(4)}$ is positive definite and therefore its determinant is positive [13]. This ensures the existence and the uniqueness of the solution.

Theorem 2 For each set of points $P_i(x_i, y_i), (n \geq 3)$ in the plane, for $C_0(C_{0x}, C_{0y}) \equiv P_0(x_0, y_0)$ and $C_3(C_{3x}, C_{3y}) \equiv P_n(x_n, y_n)$, there exist singular internal control points $C_1(C_{1x}, C_{1y})$ and $C_2(C_{2x}, C_{2y})$ of the third-order Bezier curve for which the sums $E(C_x)$ and $E(C_y)$ defined by (9) and (10) assume their minimum values.

Proof: For the coordinates of the internal control points $C_1(C_{1x}, C_{1y})$ and $C_2(C_{2x}, C_{2y})$ of the third-order Bezier curve, similar to the proof of Theorem 1, we obtain:

$$\begin{bmatrix} C_{1x} \\ C_{2x} \end{bmatrix} = S_{(3)}^{-1} \begin{bmatrix} SX_{2,1} - C_{0x}S_{5,1} - C_{3x}S_{2,4} \\ SX_{1,2} - C_{0x}S_{4,2} - C_{3x}S_{1,5} \end{bmatrix} \quad (16)$$

$$\begin{bmatrix} C_{1y} \\ C_{2y} \end{bmatrix} = S_{(3)}^{-1} \begin{bmatrix} SY_{2,1} - C_{0y}S_{5,1} - C_{3y}S_{2,4} \\ SY_{1,2} - C_{0y}S_{4,2} - C_{3y}S_{1,5} \end{bmatrix}, \quad (17)$$

where $S_{(3)} = \begin{bmatrix} 3S_{4,2} & 3S_{3,3} \\ 3S_{3,3} & 3S_{2,4} \end{bmatrix}$ is a positive definite matrix. Therefore, its determinant is positive, which guarantees the existence of the solution.

Theorem 3 For each set of points $P_i(x_i, y_i), (n \geq 2)$ in the plane, for $C_0(C_{0x}, C_{0y}) \equiv P_0(x_0, y_0)$ and $C_2(C_{2x}, C_{2y}) \equiv P_n(x_n, y_n)$, there exist singular internal control point $C_1(C_{1x}, C_{1y})$ of the second-order Bezier curve for which the sums $E(C_x)$ and $E(C_y)$ defined by (9) and (10) assume their minimum values.

Proof: For the coordinates of the internal control point $C_1(C_{1x}, C_{1y})$ of the second-order Bezier curve, analogously to the previous theorems, we obtain:

$$C_{1x} = \frac{SX_{1,1} - C_{0x}S_{3,1} - C_{2x}S_{1,3}}{2S_{2,2}} \tag{18}$$

$$C_{1y} = \frac{SY_{1,1} - C_{0y}S_{3,1} - C_{2y}S_{1,3}}{2S_{2,2}} \tag{19}$$

and with that $S_{2,2} \neq 0$ according to (8) and (11).

Remark 3 Generally, for formulas (14)-(19) it is not required that the sequence of abscisses or ordinates of the points $P_i(x_i, y_i), i = \overline{0, n}$ to be monotone.

The plane curve $B(t)$ is set parametrically and the correspondence between the abscisses and the ordinates of its points is implicit. Therefore, we will take notice of defining the ordinate of a point of the curve by a given abscissa.

Task 1. Let the curve $B(t)$ be determined by the set of points $P_i(x_i, y_i), i = \overline{0, n}$, for which $x_0 < x_1 < \dots < x_n$ and $B_x(t)$ is a strictly monotonic function of $t \in [0, 1]$. Determine the ordinate y_B at a point of the curve by the given abscissa $x_B \in [x_0, x_n]$.

Solution: We first localize the numerical interval that contains x_B . Suppose that $x_B \in [x_{i-1}, x_i]$. By linear interpolation according to the values t_{i-1} and t_i defined by (8), for t_B (Figure 2) there is obtained:

$$t_B = t_{i-1} + \frac{x - x_{i-1}}{x_i - x_{i-1}}(t_i - t_{i-1}), \quad t_B \in [0, 1], \tag{20}$$

where we calculate $y_B = B_y(t_B)$.

Determining of a α -cut of the membership function proposed in the next section is the reverse of Task 1:

Task 2. Let the curve $B(t)$ be determined by set points $P_i(x_i, y_i), i = \overline{0, n}$ for which $x_0 < x_1 < \dots < x_n$; $B_y(t) \in [0, 1]$ and $B_x(t), B_y(t)$ are strictly monotonic functions of $t \in [0, 1]$. Determine the abscissa $x_B \in [x_0, x_n]$ at a

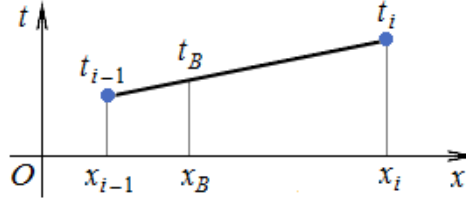


Figure 2: Linear interpolation to determine the value of t_B

point of the curve by the specified ordinate $y_B \in [0, 1]$.

Solution: Similarly to the solution of the previous task, we define:

$$t_B = t_{i-1} + \frac{y - y_{i-1}}{y_i - y_{i-1}}(t_i - t_{i-1}), \quad t_B \in [0, 1], \quad (21)$$

where:

- $y_B \in [y_{i-1}, y_i]$ if $B_y(t)$ is a monotonic increasing function of t ;
- $y_B \in [y_i, y_{i-1}]$ if $B_y(t)$ is a monotonic decreasing function of t

and $x_B = B_x(t_B)$.

4 Constructing a membership function by approximating a frequency distribution with a Bezier curve

We will use the frequency distributions for the five stages of sedation, which are published in [11] and are listed in Tables 4-8 of Appendix section.

From the corresponding table for each stage, a series of points are formed which have evenly distributed abscissas. The points coordinates $P_i(m_i, \tilde{p}_i)$, $i = \overline{1, l}$ are input data for the following algorithm:

1. Points P_0 (left) and P_{l+1} (right) with zero ordinates added to the left and right of the series of points, so that the even distribution of the points abscissas is preserved (Figure 3).
2. We determine the midpoint (m_M, \tilde{p}_M) of the class interval with a maximum frequency, i.e. $\tilde{p}_M = 1$. Let us denote $m = m_M$.
3. The series of points $P_i(m_i, \tilde{p}_i)$, $i = \overline{0, l+1}$ is divided into two groups:

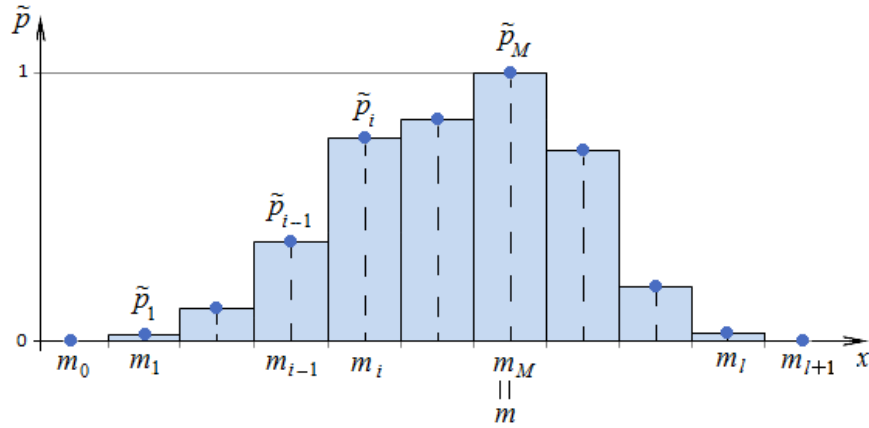


Figure 3: A histogram of the frequency distribution and used parameter markers

- left $P_i(m_i, \tilde{p}_i), i = \overline{0, M}$, containing $(M + 1)$ points, i.e. $n = M$;
 - right $P_i(m_i, \tilde{p}_i), i = \overline{M, l + 1}$, containing $(l - M + 2)$ points, i.e. $n = l - M + 1$.
4. Using the formulas given in Section 3 for the left and right group of points, we successively define left $B^L(t)$ and right $B^R(t)$ Bezier curve under the following conditions:
- (a) The number $(k + 1)$ of control points of $B(t)$ is determined by:

$$k = \begin{cases} n, & n = 2; 3 \\ 4, & n \geq 4 \end{cases} .$$

- (b) By formula (7) we define the lengths $r_i, i = \overline{1, n}$ of the segments between each two adjacent points. We set $z_i = 1, i = \overline{1, n}$.
- (c) $r_i = z_i r_i, i = \overline{1, n}$.
- (d) We calculate d_i and $t_i, i = \overline{0, n}$. Then we find the coordinates of the internal control points (Theorems 1-3) of curves $B(t)$.
- (e) We check the monotony of $B_x(t)$ and $B_y(t)$ and the non-negativity of $B_y(t)$:
- If $B_x(t)$ and $B_y(t)$ are monotonic and $B_y(t) \geq 0, t \in [0, 1]$, we move to step 5 of the algorithm;

- For each interval $[t_{i-1}, t_i]$ in which $B_x(t)$ or $B_y(t)$ is not a monotonic function or $B_y(t) < 0$, the value of z_i is reduced by half:

$$z_i = \begin{cases} z_i, & \text{if } B_x(t) \text{ and } B_y(t) \geq 0 \text{ are monotonic in } [t_{i-1}, t_i] \\ \frac{1}{2}z_i, & \text{otherwise.} \end{cases}$$

We return to step 4 (c) of the algorithm.

5. We construct the membership function from the two parametrically defined curves:

$$\mu_A(x(t), y(t)) = \begin{cases} \begin{cases} x = B_x^L(t) \\ y = B_y^L(t) \end{cases}, & t \in [0, 1], \text{ where } x \leq m \\ \begin{cases} x = B_x^R(t) \\ y = B_y^R(t) \end{cases}, & t \in [0, 1], \text{ where } x > m \end{cases} \quad (22)$$

and build it.

Following the algorithm, for each of the five sedation stages the coordinates of the control points of Bezier's curves are calculated (Table 9 in the Appendix section) and the membership functions are built (Figures 4-8, in black). The convexity of the constructed fuzzy numbers is guaranteed in step 4 (e) of the algorithm by the requirement for monotonicity of the obtained Bezier curves. Adding points P_0 and P_{l+1} with zero ordinates in step 1 of the algorithm provides $support(A)$ to be bounded.

5 Comparing the results and conclusion

Nasibov and Peker [11] compared the classification accuracy based on exponential membership functions (3) and Gaussian membership functions (2).

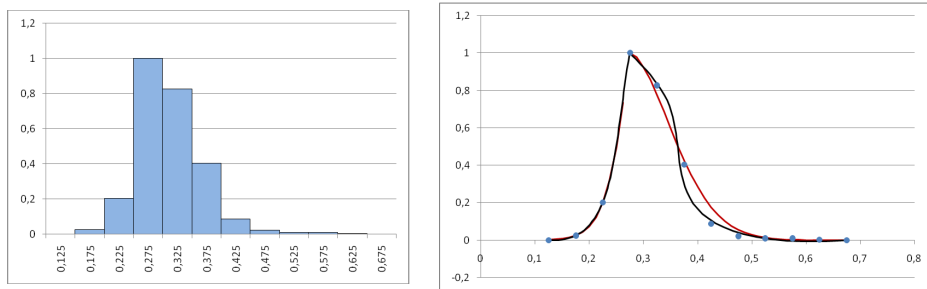


Figure 4: A histogram and membership functions of first sedation stage

They conclude that the average degree of classification accuracy of (3) is higher than that of (2). Since we do not have the necessary data to compare the classification accuracy of the proposed functions (22) and the functions (3), we will only compare them by the sum of the squares of the deviations from the points.

The curves that we will compare are shown on Figures 4-8, where:

- The functions in black correspond to (22) and are built according to the algorithm in Section 4. The control points are listed in Table 9 in the Appendix section.
- The functions in red (or gray in the gray scale) correspond to (3) and are constructed according to the analytical type and the parameter values specified in [11]. The parameter values are listed in Table 10 in the Appendix section.

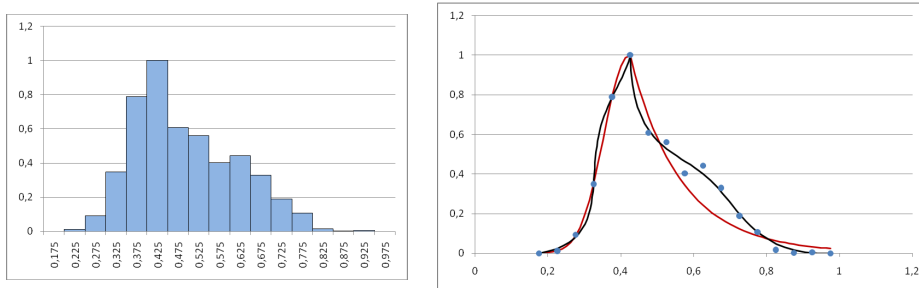


Figure 5: A histogram and membership functions of second sedation stage

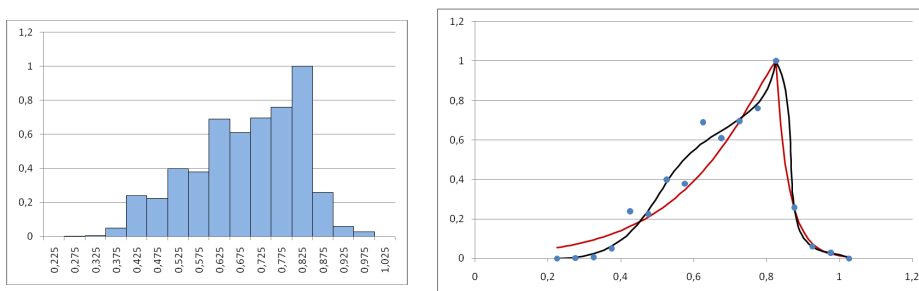


Figure 6: A histogram and membership functions of third sedation stage

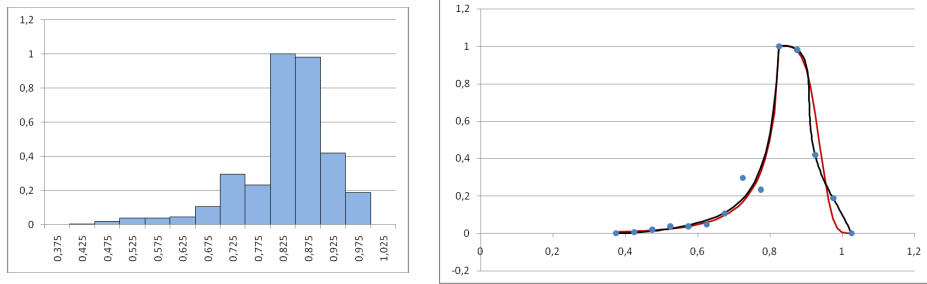


Figure 7: A histogram and membership functions of fourth sedation stage

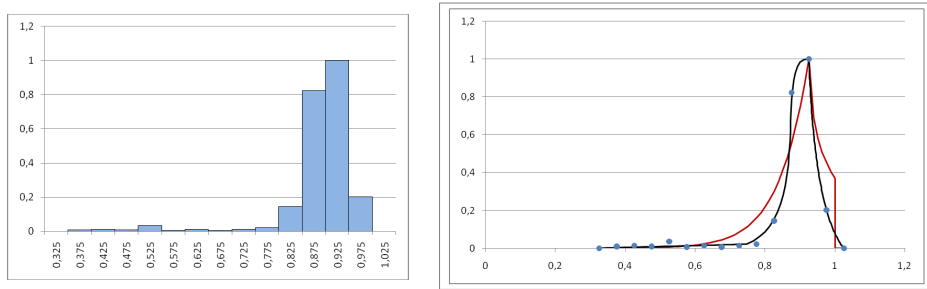


Figure 8: A histogram and membership functions of fifth sedation stage

Functions (22) are defined parametrically, but functions (3) are clearly defined. This determines the difference in the measurement of the deviations of the curves from the frequency distribution points. The deviations of curves (22) must be reported on both coordinate axes, while the deviations of the curves (3) are defined as deviations only on the ordinate axis. The formulas for sum of squares deviations on which the values of Table 2 are calculated are:

- for (22): $E_{(22)}(\tilde{p}_i, \mu_A) = \sum_{i=0}^{l+1} [(m_i - B_x(t_i))^2 + (\tilde{p}_i - B_y(t_i))^2]$;
- for (3): $E_{(3)}(\tilde{p}_i, \mu_A) = \sum_{i=0}^{l+1} (\tilde{p}_i - \mu_A(m_i))^2$.

The result of comparing the mean values of $E(\tilde{p}_i, \mu_A)$ for both methods with a level of significance $\alpha = 0,05$ are shown in Table 3. The t_{Stat} value falls into the critical area $(-2,82849 < -2,13185)$ of the null hypotheses $H_0 : E_{(22)} \geq E_{(3)}$ against its alternative $H_1 : E_{(22)} < E_{(3)}$, which means that the $E_{(22)}$ values are significantly smaller than those of $E_{(3)}$.

Stages of sedation	$E_{(22)}(\tilde{p}_i, \mu_A)$	$E_{(3)}(\tilde{p}_i, \mu_A)$
1	0,0013931	0,0121480
2	0,0063041	0,0903728
3	0,0163010	0,1154965
4	0,0102372	0,0880298
5	0,0024799	0,2297327

Table 2: Sum of squares deviations

	$E_{(22)}$	$E_{(3)}$
Mean	0,00734306	0,10715596
Variance	3,71881E-05	0,006192155
Observations	5	5
df	4	
t Stat	-2,828491142	
P(T ≤ t) one-tail	0,023708788	
t Critical one-tail	2,131846782	
P(T ≤ t) two-tail	0,047417576	
t Critical two-tail	2,776445105	

Table 3: *t*-Test: Paired Two Sample for Means

By the *t*-criterion we have established that the membership functions (22) are closer to the frequency distribution points compared to the membership functions (3). This gives us a reason to consider (22) a good alternative to (3) and with that each of these two methods has advantages and disadvantages. In some cases, a disadvantage of the proposed membership function (22) may be its "sensitivity" to fluctuations in frequency distribution. The key to overcoming this "sensitivity" is step 4 (e) of the algorithm. Refining the values that are assigned to z_i would improve the algorithm and may be subject to future research.

Studies based on the values of the bispectral index are used in various sociological and marketing studies [4, 14]. The derived formulas for defining Bezier curves, which best describe a series of points, could be used as an analogue of exponential smoothing, and the proposed algorithm for designing membership functions can be used to solve a wide range of problems, including financial, marketing, macro- and microeconomic problems [6, 2, 8, 9], etc.

References

- [1] L. C. de Barros, R. C. Bassanezi, W. A. Lodwick. *A First Course in Fuzzy Logic, Fuzzy Dynamical Systems, and Biomathematics*, Studies in Fuzziness and Soft Computing. Springer-Verlag Berlin Heidelberg, 2017.
- [2] V. Chernov, O. Dorokhov, L. Dorokhova, V. Chubuk. Using Fuzzy Logic for Solution of Economic Tasks: Two Examples of Decision Making under Uncertainty. *Montenegrin Journal of Economics*, 11(1): 85-100, 2015.
- [3] S. Feng, H. Li, D. Hu. A new training algorithm for HHFNN based on Gaussian membership function for approximation. In *Neurocomputing*, 72:1631-1638, 2009.
- [4] I. Guler, E. Ubeyli. Adaptive neuro-fuzzy inference system for classification of EEG signals using wavelet coefficients. *Journal of Neuroscience Methods*, 148(2): 113-121, 2005.
- [5] T. Hasuike, H. Katagiri, H. Tsubakic. A constructing algorithm for appropriate piecewise linear membership function based on statistics and information theory. *Procedia Computer Science*, 60: 994-1003, 2015.
- [6] M. G. Iskander. Exponential Membership Functions in Fuzzy Goal Programming: A Computational Application to a Production Problem in the Textile Industry. *American Journal of Computational and Applied Mathematics*, 5(1): 1-6, 2015.
- [7] J.-S. R. Jang, C.-T. Sun, E. Mizutani. *Neuro-Fuzzy and Soft Computing: A Computational Approach to Learning and Machine Intelligence*. Prentice-Hall, 1997.
- [8] S. Jain, M. Khare. Construction of fuzzy membership functions for urban vehicular exhaust emissions modeling. *Environ Monit Assess*, 167: 691-699, 2010.
- [9] G. Maniu. The Construction of the Membership Functions in the Fuzzy Measuring of Poverty. *Bulletin of the Petroleum-Gas University of Ploiesti*, Economic Sciences Series, 61(1): 107-117, 2009.
- [10] E. Nasibov, G. Ulutagay. Comparative clustering analysis of bispectral index series of brain activity. *Expert Systems with Applications*, 37: 2495-2504, 2010.

- [11] E. Nasibov, S. Peker. Exponential Membership Function Evaluation based on Frequency. *Asian Journal of Mathematics and Statistics* 4(1): 8-20, 2011.
- [12] T. J. Ross. *Fuzzy Logic with Engineering Applications*, Second edition. John Wiley and Sons Ltd, 2004.
- [13] N. A. Suleiman. Least squares data fitting with quadratic Bezier curves. In *Proceedings of the YSU*, Series Physical and Mathematical sciences, (2): 42-49, 2013.
- [14] M. Tsutsumi, H. Nogaki, Y. Shimizu, T. E. Stone, T. Kobayashi. Individual reactions to viewing preferred video representations of the natural environment: A comparison of mental and physical reactions. *Japan Journal of Nursing Science*, 14: 3-12, 2017.
- [15] D. Viattchenin, R. Tati, A. Damaratski. Designing Gaussian Membership Functions for Fuzzy Classifier Generated by Heuristic Possibilistic Clustering. *Journal of Information and Organizational Sciences*, 37(2): 127-139, 2013.
- [16] T.-P. Wu and S.-M. Chen. A New Method for Constructing Membership Functions and Fuzzy Rules from Training Examples. *IEEE Transactions on Systems, Man, and Cybernetics*, part B: Cybernetics, 29(1): 25-40, 1999.
- [17] C. C. Yang, N. K. Bose. Generating fuzzy membership function with self-organizing feature map. In *Pattern Recognition Lett.*, 27: 356-365, 2006.
- [18] H.-J. Zimmermann. Fuzzy set theory. *WIREs Computational Statistics*, 2: 317-332, 2010.

A Appendix

Class interval	Midpoint m_i	Frequency f_i	Relative frequency p_i	Normalized frequency \tilde{p}_i
[0, 15; 0, 2)	0,175	8	0,00960384	0,02484472
[0, 2; 0, 25)	0,225	65	0,07803121	0,201863354
[0, 25; 0, 3)	0,275	322	0,38655462	1
[0, 3; 0, 35)	0,325	266	0,31932773	0,826086957
[0, 35; 0, 4)	0,375	130	0,15606242	0,403726708
[0, 4; 0, 45)	0,425	28	0,03361345	0,086956522
[0, 45; 0, 5)	0,475	7	0,00840336	0,02173913
[0, 5; 0, 5)5	0,525	3	0,00360144	0,00931677
[0, 55; 0, 6)	0,575	3	0,00360144	0,00931677
[0, 6; 0, 65)	0,625	1	0,00120048	0,00310559

Table 4: Frequency table of first sedation stage

Class interval	Midpoint m_i	Frequency f_i	Relative frequency p_i	Normalized frequency \tilde{p}_i
[0, 2; 0, 25)	0,225	4	0,00229621	0,011267606
[0, 25; 0, 3)	0,275	33	0,01894374	0,092957746
[0, 3; 0, 35)	0,325	124	0,07118255	0,349295775
[0, 35; 0, 4)	0,375	280	0,16073479	0,788732394
[0, 4; 0, 45)	0,425	355	0,20378875	1
[0, 45; 0, 5)	0,475	216	0,12399541	0,608450704
[0, 5; 0, 55)	0,525	199	0,11423651	0,56056338
[0, 55; 0, 6)	0,575	143	0,08208955	0,402816901
[0, 6; 0, 65)	0,625	157	0,09012629	0,442253521
[0, 65; 0, 7)	0,675	117	0,06716418	0,329577465
[0, 7; 0, 75)	0,725	67	0,03846154	0,188732394
[0, 75; 0, 8)	0,775	38	0,02181401	0,107042254
[0, 8; 0, 85)	0,825	6	0,00344432	0,016901408
[0, 85; 0, 9)	0,875	1	0,00057405	0,002816901
[0, 9; 0, 95)	0,925	2	0,00114811	0,005633803

Table 5: Frequency table of second sedation stage

Class interval	Midpoint m_i	Frequency f_i	Relative frequency p_i	Normalized frequency \tilde{p}_i
[0, 25; 0, 3)	0,275	1	0,0003712	0,002004008
[0, 3; 0, 35)	0,325	3	0,00111359	0,006012024
[0, 35; 0, 4)	0,375	25	0,00927988	0,0501002
[0, 4; 0, 45)	0,425	119	0,04417223	0,238476954
[0, 45; 0, 5)	0,475	112	0,04157387	0,224448898
[0, 5; 0, 55)	0,525	199	0,07386785	0,398797595
[0, 55; 0, 6)	0,575	189	0,0701559	0,378757515
[0, 6; 0, 65)	0,625	344	0,12769117	0,689378758
[0, 65; 0, 7)	0,675	304	0,11284336	0,609218437
[0, 7; 0, 75)	0,725	347	0,12880475	0,695390782
[0, 75; 0, 8)	0,775	379	0,140683	0,759519038
[0, 8; 0, 85)	0,825	499	0,18522643	1
[0, 85; 0, 9)	0,875	129	0,04788419	0,258517034
[0, 9; 0, 95)	0,925	30	0,01113586	0,06012024
[0, 95; 1)	0,975	14	0,00519673	0,028056112

Table 6: Frequency table of third sedation stage

Class interval	Midpoint m_i	Frequency f_i	Relative frequency p_i	Normalized frequency \tilde{p}_i
[0, 4; 0, 45)	0,425	1	0,00135685	0,00456621
[0, 45; 0, 5)	0,475	4	0,00542741	0,01826484
[0, 5; 0, 55)	0,525	8	0,01085482	0,03652968
[0, 55; 0, 6)	0,575	8	0,01085482	0,03652968
[0, 6; 0, 65)	0,625	10	0,01356852	0,0456621
[0, 65; 0, 7)	0,675	23	0,0312076	0,105022831
[0, 7; 0, 75)	0,725	65	0,08819539	0,296803653
[0, 75; 0, 8)	0,775	51	0,06919946	0,232876712
[0, 8; 0, 85)	0,825	219	0,29715061	1
[0, 85; 0, 9)	0,875	215	0,2917232	0,98173516
[0, 9; 0, 95)	0,925	92	0,12483039	0,420091324
[0, 95; 1)	0,975	41	0,05563094	0,187214612

Table 7: Frequency table of fourth sedation stage

Class interval	Midpoint m_i	Frequency f_i	Relative frequency p_i	Normalized frequency \tilde{p}_i
[0, 35; 0, 4)	0,375	3	0,00413223	0,009493671
[0, 4; 0, 45)	0,425	4	0,00550964	0,012658228
[0, 45; 0, 5)	0,475	3	0,00413223	0,009493671
[0, 5; 0, 55)	0,525	11	0,01515152	0,034810127
[0, 55; 0, 6)	0,575	2	0,00275482	0,006329114
[0, 6; 0, 65)	0,625	4	0,00550964	0,012658228
[0, 65; 0, 7)	0,675	2	0,00275482	0,006329114
[0, 7; 0, 75)	0,725	4	0,00550964	0,012658228
[0, 75; 0, 8)	0,775	7	0,00964187	0,022151899
[0, 8; 0, 85)	0,825	46	0,06336088	0,14556962
[0, 85; 0, 9)	0,875	260	0,35812672	0,82278481
[0, 9; 0, 95)	0,925	316	0,43526171	1
[0, 95; 1)	0,975	64	0,08815427	0,202531646

Table 8: Frequency table of fifth sedation stage

Stages	Left		Right	
	σ	S_L	β	S_R
1	0,03366153	1,19058453	0,10954908	1,75612535
2	0,098304385	2,12921635	0,140004284	0,97277506
3	0,23903161	1,16559615	0,03494202	0,91429043
4	0,04244326	0,67457267	0,12082079	4,33694334
5	0,08407821	1,03766617	0,075	0,55743699

Table 10: Parameters of the membership functions (3) used as a benchmark

Stages	C_i	Left		Right	
		x	y	x	y
1	C_0	0,125	0	0,275	1
	C_1	0,247991904	-0,021264839	0,385177558	0,698654314
	C_2	0,242565841	0,430096798	0,401145303	0,52556588
	C_3	0,275	1	0,243719602	-0,07293049
	C_4			0,675	0
2	C_0	0,175	0	0,425	1
	C_1	0,446856004	0,081682191	0,432350881	0,162518
	C_2	0,228966718	0,606975012	0,782069858	0,768679
	C_3	0,378416281	0,700014982	0,585874127	-0,02454
	C_4	0,425	1	0,975	0
3	C_0	0,225	0	0,825	1
	C_1	0,624874518	-0,002210513	0,919899079	0,681197
	C_2	0,4019694	0,85309558	0,793213422	-0,11791
	C_3	0,784104357	0,444195245	0,945898462	0,087821
	C_4	0,825	1	1,025	0
4	C_0	0,375	0	0,825	1
	C_1	0,543533011	-0,006419047	1,000155204	1,038217807
	C_2	0,709677477	0,133690305	0,816868712	0,414115227
	C_3	0,797493323	0,004591904	0,966205507	0,293372071
	C_4	0,825	1	1,025	0
5	C_0	0,325	0	0,925	1
	C_1	0,548083099	0,217777331	0,940176064	0,188264274
	C_2	1,080709167	-0,688340048	1,025	0
	C_3	0,768476768	1,035569291		
	C_4	0,925	1		

Table 9: Coordinates of control points